

3-3-2 Different Behaviors of TEC and NmF2 Observed During Large Geomagnetic Storms

JIN Hidekatsu and MARUYAMA Takashi

We investigated behaviors of ionospheric total electron content (TEC) and F2 peak electron density (NmF2) observed at midlatitudes during geomagnetic storms. Although TEC and NmF2 disturbances were similar during moderate storms, they were sometimes quite different during severe storms. By using numerical simulation, we suggest that different TEC and NmF2 disturbances can be caused by effects of F-region plasma dynamics enhanced when storm drivers operate suddenly or effects of more than one storm drivers operating simultaneously. Therefore, observations of such TEC and NmF2 disturbances include important information on the plasma dynamics in the F region and on the operating storm drivers.

Keywords

Ionosphere, TEC, foF2, Magnetic storm, Simulation

1 Introduction

Ionospheric density distributions are not constant and could vary not only day to day but also seasonally and during different periods of solar activity (cycles of about 11 years). Apart from regular variations, part of the energy of a magnetic storm resulting from an explosive event (flare) on the solar surface will penetrate the ionosphere and generate irregular ionospheric density disturbances. Given the growing popularity of satellite positioning based on GPS satellites in modern society, ionospheric density disturbances? a major source of satellite positioning error? could pose a significant obstacle to that function. Studies are now underway to probe into the mechanism of generating ionospheric disturbances and to forecast those disturbances.

Various processes can drive ionospheric disturbances. The most commonly known processes are as follows:

- (1) Penetration of magnetospheric electric field

The magnetosphere exists outside the

ionosphere, and over the polar regions both the magnetosphere and ionosphere are interconnected by magnetic field lines. The electric field associated with the motion of magnetospheric plasma normally acts only on the ionosphere in the polar regions, but could penetrate into the ionosphere in low- and mid-latitude regions from the polar regions during magnetic storms. This penetration electric field drives the motion of ionospheric plasma, thereby leading to density disturbances.

- (2) Changes in thermospheric circulation
Particles precipitating along the magnetic field lines from the magnetosphere heat the thermosphere over the polar regions, and thus disturb global atmospheric circulation. Because the thermospheric motion drags the ionospheric plasma directed along the magnetic field lines, changes in atmospheric circulation would lead to density disturbances.
- (3) Changes in the thermospheric compo-

sition

The heated thermosphere over the polar regions as mentioned in (2) expands the earth's atmosphere, and thereby elevates relatively heavy molecules. Such molecules flowing into low- and mid-latitude regions will promote chemical reactions for ions to induce diminishing ionospheric density.

In addition to the processes described in (1) to (3) above, disturbance in the ionospheric dynamo (as explained in Reference [1]) and traveling atmospheric/ionospheric disturbances generated in the polar regions may also be at work. (To find out more, see Reference [2] and other references.) Note that the ionospheric disturbances actually observed during major magnetic storms appear so complicated that it is difficult to understand how the disturbance processes described above contribute to actually observed ionospheric disturbances. Moreover, disturbances vary phase by phase, making the work of identifying the prevalent disturbance process and under what conditions a key research challenge.

This study examines the behavior of the ionospheric total electron content (TEC) observed in Japan and the maximum F-region electron density (NmF2) in an effort to under-

stand the mechanism of generating ionospheric disturbances. NmF2 is the maximum value of electron density in its height distribution. NmF2 is determined from the F2 region critical frequency observed by ionosondes. TEC is the value of electron density integrated in height as calculated by implementing the algorithm reported in Reference [3]. Because the high-density F2 region contributes most to TEC, both TEC and NmF2 normally exhibit identical day-to-day variations. Figure 1 shows the correlation between variations in TEC and NmF2 as observed at ionosonde observatories (from north to south, at Wakkanai, Kokubunji, Yamagawa and Okinawa). While the Kp index—an indicator of the degree of geomagnetic disturbance—remains not noticeably high (at $K_p < 6$), the straight lines that represent the relations between variations in TEC and NmF2 essentially pass the origin, showing basically similar slopes. Once a large magnetic storm occurs ($K_p > 6$), however, the slopes that determine the correlation between variations in TEC and those in NmF2 move away the origin, unlike in the case of $K_p < 6$. This amounts to the differences between the behaviors of TEC and NmF2. This paper introduces some typical observations and reports an analysis of the probable causes of such behavioral differences. The

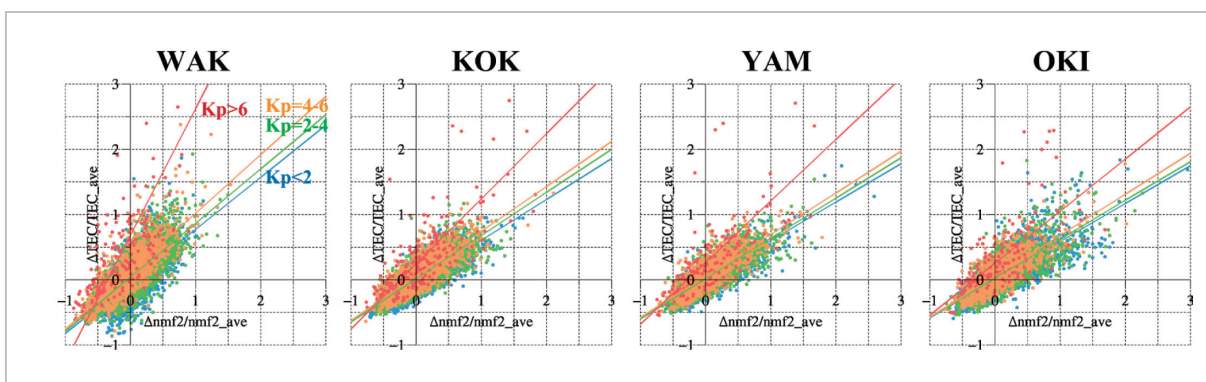


Fig. 1 Correlation between variations in TEC and NmF2 as observed at domestic ionosonde observatories

Correlation between variations in TEC and NmF2 as observed at Wakkanai (WAK), Kokubunji (KOK), Yamagawa (YAM), and Okinawa (OKI). The observation period is from 2002 to 2006 for Yamagawa (YAM) and from 2001 to 2006 for other sites. Each data point denotes an hourly average; deviations from the monthly average are normalized by the monthly average. Each size of the Kp index—an indicator of the degree of geomagnetic disturbance—is marked in a different color.

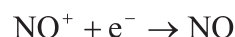
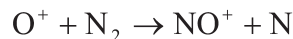
report also shows that behavioral differences between TEC and NmF2 offer clues to understanding the dynamics of the F-region plasma during a magnetic storm, and the processes that have driven ionospheric disturbances.

2 TEC and NmF2 observations

2.1 Ionospheric disturbances during moderate magnetic storms

This section begins by introducing typical observations of TEC and NmF2 during moderate magnetic storms. Figure 2 (a) shows hourly changes in TEC and NmF2 observed at Wakkanai for six days (starting from April 17), along with Dst as an indicator of magnetic storm scale. Dst began to decline starting from about the 18th day, Japan Standard Time (JST), with magnetospheric disturbances lasting about five days. During this period, TEC and NmF2 significantly declined from their monthly medians twice (on the 19th and 21st days), and such phenomenon is so-called negative storm. Both TEC and NmF2 declined by

40 to 60% and exhibit similar time-dependent changes. The negative storm may be caused by changes in the thermosphere that increased molecular components, resulting in a reduction of O^+ (a dominant ion component in the F-region) through the promotion of these chemical reactions.



The occurrence of thermospheric disturbance is supported by an observation of increased neutral atmospheric mass by Germany's CHAMP satellite orbiting at an altitude of about 400 km during the same period [4].

Next, Fig. 2 (b) presents observational data of Dst, TEC and NmF2, over a three-day period starting on April 13, 2006. Dst declined on the 14th day, reaching about -100 nT when TEC and NmF2 rose to about twice their monthly medians, and such phenomenon is so-called positive storm. Thus, two probable causes of positive storm are the penetration of

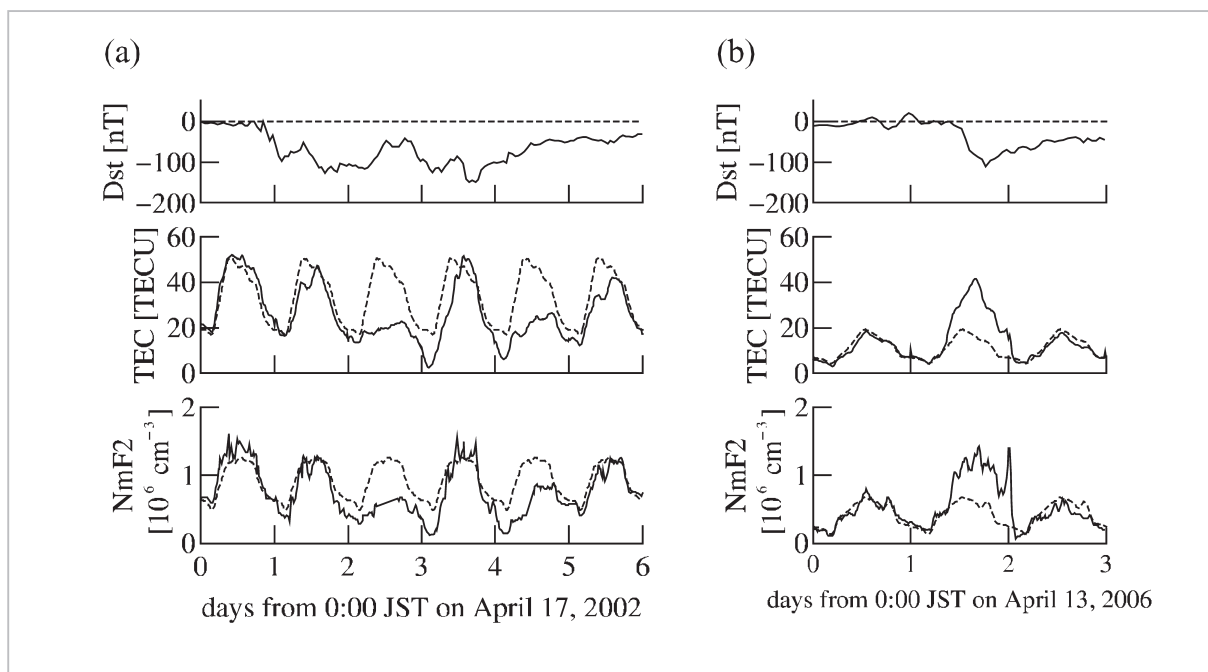


Fig.2 Observations of ionospheric disturbances during moderate magnetic storms

From top to bottom: time-dependent changes in DST, TEC and NmF2. (a) Data observed at Wakkanai from April 17 to 22, 2002; (b) Data observed at Kokubunji from April 13 to 15, 2006. In both panels, each dotted line marks a monthly median given for the sake of comparison.

magnetospheric electric field and the change in thermospheric circulation as described in the preceding chapter. In the former case, an enhanced eastward electric field induces a movement of ionospheric plasma in the direction perpendicular to the magnetic field lines (upward/poleward), whereas in the latter case the thermospheric neutral wind being accelerated toward the equator drags the ionospheric plasma upward along the magnetic field lines. Rises in ionospheric height cause changes in the density and composition of the ambient atmosphere, and result in reductions in the molecular components of ionospheric plasma—a situation opposite that in the case of a negative storm. Consequently, fewer O^+ ions are lost due to chemical reactions, thereby increasing the density. In this event, TEC and NmF2 also exhibit increases to nearly the same extent and similar time-dependent changes.

2.2 Ionospheric disturbances during large magnetic storms

Next, several example observations of TEC and NmF2 during relatively large magnetic storm are shown. Figure 3 shows time-dependent changes in Dst, TEC and NmF2 over a two-day period starting on November 7, 2004. Values observed at Wakkanai (36.6° N magnetic latitude) and those observed at Kokubunji (26.8° N magnetic latitude) are represented by red and black lines, respectively. Dst began to decline starting on the 8th day, reaching about -400 nT. This magnetic storm was found to be much larger than the two magnetic storms exemplified in Fig. 2. TEC and NmF2 showed a positive disturbance occurring on the 8th day, and lasting through the daytime and after the sunset at Kokubunji. Disturbance became different between TEC and NmF2 at Kokubunji, with TEC reaching a level about six times higher than the monthly average in the daytime when compared with NmF2, which reached a maximum level of about three times higher. Behavioral differences between TEC and NmF2 were more pronounced at Wakkanai, such as increased

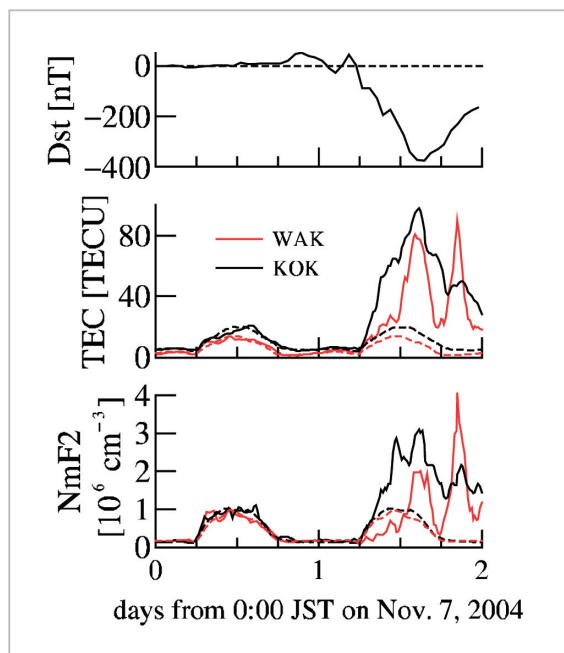


Fig.3 Observation of ionospheric disturbances during large magnetic storm 1

DST index and observational data of TEC and NmF2 obtained at Wakkanai (red line) and Kokubunji (black line). The data period is November 7 to 8, 2004.

TEC on the morning of the 8th day, while NmF2 conversely decreased from its monthly average and then increased in the afternoon. Differences in disturbances between Wakkanai and Kokubunji are also significant. At Wakkanai, noticeable peaks appeared in TEC (and in NmF2 as well) in the daytime and after sunset. At Kokubunji, peaks were also observed after the sunset, though smaller than those observed at Wakkanai. Peaks observed after the sunset are interpreted as a phenomenon called “SED” [5].

Figure 4 (a) shows Dst observed on November 6, 2001, as another example of a large magnetic storm, along with NmF2, hpF2 (ionospheric height at which the F2 region density peaks), and TEC at Wakkanai. In this example, Dst began to decline starting at about 11:00 JST and, at about the same time, both TEC and hpF2 increased. Conversely, NmF2 began decreasing and then increased about two hours later at 13:00 JST. In this way, TEC and NmF2 exhibited totally oppo-

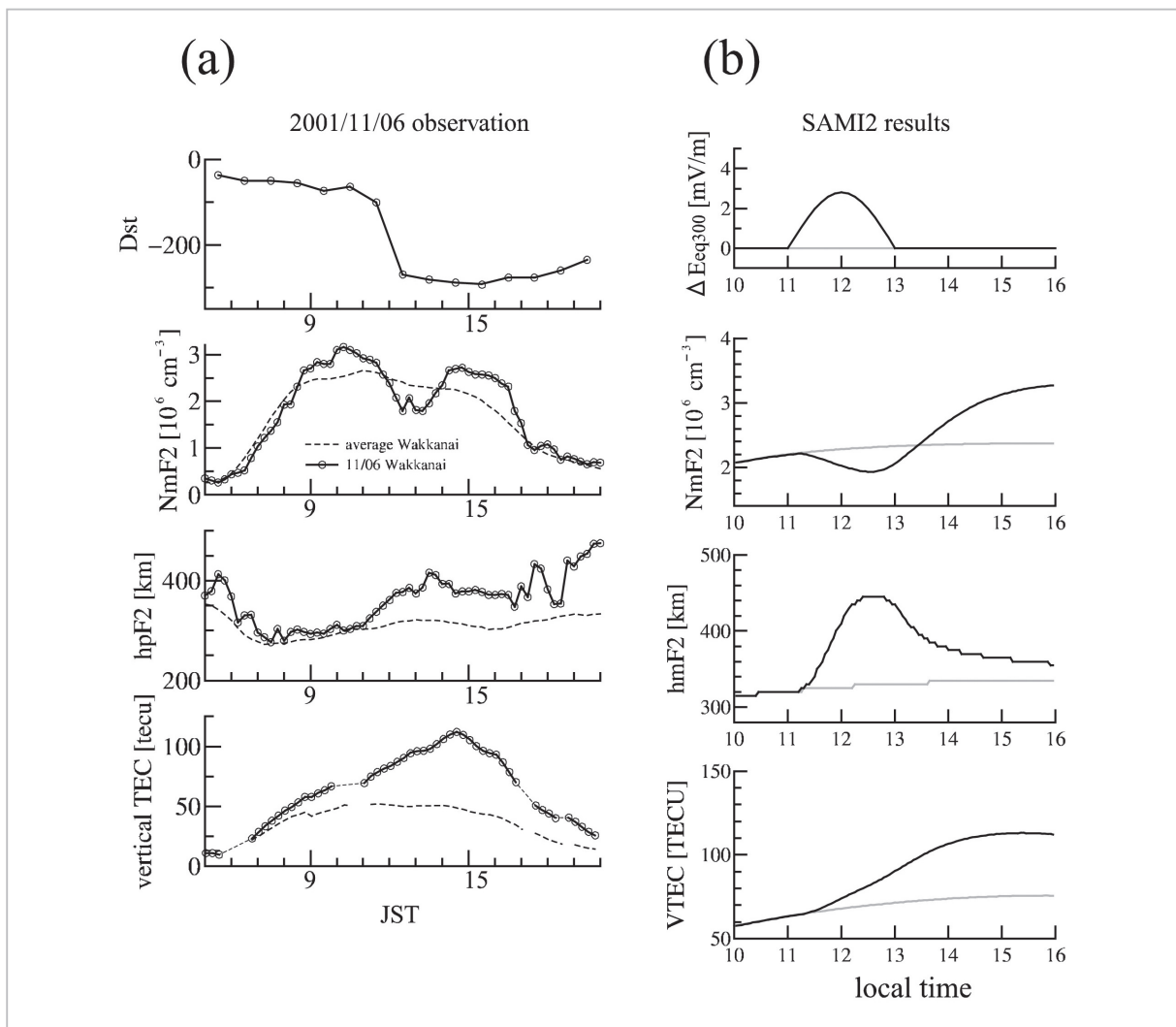


Fig.4 Observation of ionospheric disturbances during large magnetic storm, and reproduction through numerical simulation

(a) Dst index observed on November 6, 2001, along with NmF2, hpF2 and TEC at Wakkanai. (b) From the top, electric field input to SAMI2 (at ionospheric height of 300 km on the magnetic equator, with eastward electric field difference from the background electric field taken as positive), calculated NmF2, hmF2 and TEC at Wakkanai. The gray line points to variations obtained in the quiescent time (without an electric field at work) [8].

site changes at the timing of a decrease in Dst. Another observation confirmed that the equatorial ionization anomaly spreading in the polar direction during the same time period [6] most likely resulted from enhanced eastward electric field acting on the ionosphere. (Reference [1] describes the relation between the electric field and the equatorial ionization anomaly.) The rise in hpF2 shown in Fig. 4 (a) may have been caused by this eastward electric field. In this event, TEC showed a general increase above Japan, with a reduction in NmF2 only observed at Wakkanai among the

four Japanese ionosonde observatories (from north to south, at Wakkanai, Kokubunji, Yamagawa and Okinawa) [7].

3 Discussions on different TEC and NmF2 behaviors

This chapter discusses the probable causes of different TEC and NmF2 behavior during large magnetic storms. Figure 4 (b) presents a numerical simulation that reproduces a simultaneous increase in TEC and decrease in NmF2 (similar to the observation in Fig. 4

(a)), following a penetration of magnetospheric electric field into the ionosphere [8]. An ionospheric numerical model (SAMI2 [9]) developed at the U.S. Naval Research Laboratory is used as the simulation model. The first panel in Fig. 4 (b) from the top represents time-dependent changes in electric field input to the model (i.e., difference from the background electric field). The input electric field was designed to increase eastward starting at 11:00 (in local time), peak at 12:00, and then vanish at 13:00. The peak had a size of 2.8 mV/m at an ionospheric height of 300 km above the magnetic equator, corresponding to a large magnetic storm. The second to fourth panels in Fig. 4 (b) contain the results of a simulation run in association with the input electric field in the first panel, plotting time-dependent changes in NmF2, hmF2 and TEC above Wakkanai. (The gray line points to variations obtained without an electric field at work during the magnetic storm being applied.) Time-dependent changes in hmF2 reveal that the F-region plasma rose under the influence of an eastward electric field starting at 11:00, peaked (at a difference of 120 km from the quiescent time) shortly before extinction of the input eastward electric field, and then slowly fell upon diffusion. NmF2 temporarily decreased for about two hours since 11:00, and then increased. Conversely, TEC increased monotonously past 11:00. The simulation was found to reproduce the changing trends in hmF2, NmF2 and TEC as compared to the observations shown in Fig. 4 (a), except for some mismatching in quantitative terms. The increase in hmF2 and decrease in NmF2 as observed were approximately 90 km and 40%, respectively, when compared to 110 km and 20% or so as simulated. However, configuring the simulation to have higher plasma temperature before applying an electric field would expand the decrease in NmF2 associated with the same input electric field (with a narrowing rise in hmF2), thereby approaching the observed value. In this observation event, the ionosphere may have been left in a state different from the quiescent time and prior to

penetration of the electric field, under the influence of another source of disturbance.

Figure 5 (a) shows ionospheric height distributions of the electron density immediately after the penetration of eastward electric field shown in the sample calculation in Fig. 4 (b). Likewise, Fig. 5 (b) shows the electron flux of magnetic field lines. In both diagrams, the ionospheric height relative to hmF2 is taken as the y-axis. As Fig. 5 (a) shows, the electron density is found to decrease from the quiescent time in the vicinity of the peak density, but conversely increases at heights below the peak. At a fixed ionospheric height, the ionosphere is replaced by lower-density layers at heights below the peak as it rises. Since the neutral atmosphere has higher density at lower heights, allowing the photochemical reaction to progress faster enables the electron density to quickly revert to the original density at a height below the peak. The electron density rises relative to hmF2 at heights below the peak as shown in Fig. 5 (a). This mainly contributes to increasing TEC immediately after the penetration of electric field. In contrast, the effects of plasma motion at heights above

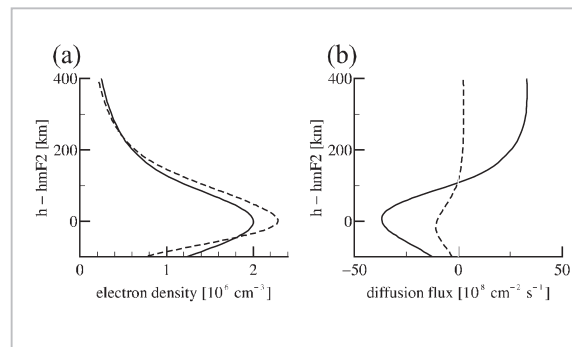


Fig.5 Ionospheric height distributions of electron density immediately after the penetration of eastward electric field

after the penetration of eastward electric field SAMI2-calculated ionospheric height distributions of electron density (a) and electron flux (b) (at Wakkanai). Each continuous line (dotted line) denotes the result of a calculation with (or without) an eastward electric field at work. The flux is a component aligned with the magnetic field lines and is taken as positive when facing upward. The height relative to hmF2 is taken as the y axis [8].

the peak exceed the effects of photochemical reaction after the height rises. Figure 5 (b) also shows increased electron flux along the magnetic field lines, as the rising height has reduced the collision frequencies between ions and the neutral atmosphere, thus promoting the diffusion of plasma along the magnetic field lines. The diffusing flux reduces the electron density in the vicinity of the F-region peak. In addition to the increased electron flux along the magnetic field lines, an electric field drift perpendicular to the magnetic field lines (poleward/upward) has the effect of increasing the volume of the magnetic tube and thus reducing the plasma density. Several hours after NmF2 decrease, photochemical reaction begins to contribute more to an increase in NmF2.

The behavioral differences between TEC and NmF2 may also be attributable to a compounded effect of the simultaneous action of multiple sources driving ionospheric disturbances. The event observed during the magnetic storm on November 8, 2004, might be one example of this effect. According to this event, TEC and NmF2 increased in a low-latitude region in Japan starting from the dawn of the eighth day, accompanied by an increase in hpF2 as well. This is considered as a positive storm caused by, for example, a penetration of magnetospheric electric field.

At Wakkanai, TEC and hpF2 increased while NmF2 temporarily remained low since the dawn as compared to the quietest time. Since the reduction in NmF2 lasted about six hours, this might well not be the effect of the mechanism as explained in Fig. 4 (b) or in Fig. 5 (effect of plasma motion temporarily exceeding the effect of photochemical reaction). Instead, the synergetic effect of a molecular component-rich atmosphere flowing from the polar regions at night to reach a high latitude in Japan, or a process inducing a negative storm and a penetrating electric field inducing a positive storm may be the causes.

4 Conclusions

This paper introduced some typical observations of TEC and NmF2 behavior during magnetic storms. During moderate magnetic storm, both TEC and NmF2 tend to exhibit similar time-dependent variations. But during larger magnetic storms, TEC and NmF2 could behave quite differently. There are several conceivable causes for these behavioral differences between TEC and NmF2. For example, when a process that drives ionospheric disturbances, such as a penetration of magnetospheric electric field, acts quickly on the ionosphere, the effect of plasma motion temporarily exceeds the effect of photochemical reaction in the vicinity of the F-region peak, while the effect of photochemical reaction prevails on the bottomside of the F-region, resulting in different variations between TEC and NmF2. Moreover, when a positive disturbance and a negative disturbance (as driving sources) act on the ionosphere simultaneously, TEC and NmF2 could vary differently. Accordingly, the observations of TEC and NmF2 not only play a mutually complementary role at geomagnetic quietest time but also obtain detailed information on the driving sources for ionospheric disturbances from a mix of TEC and NmF2 at times of geomagnetic disturbances, thereby offering clues to understanding the conditions of such phenomena and contributing to future forecasting.

Acknowledgements

This work was conducted using an ionospheric numerical model (SAMI2) developed at the U.S. Naval Research Laboratory. The World Data Center for Geomagnetism at Kyoto University provided the Dst index data. We wish to express our deepest thanks to all those involved at these institutions.

References

- 1 H. Jin, "Ionospheric Dynamo Process," Special issue of this NICT Journal, 2-3-7, 2009.
- 2 G. W. Pross, "Ionospheric F-region storms," Handbook of Atmospheric Electrodynamics, edited by H. Volland, CRC Press, Chapter 8, pp.195–248, 1995.
- 3 G. Ma and T. Maruyama, "Derivation of TEC and estimation of instrumental biases from GEONET in Japan," Ann. Geophysicae, Vol. 21, pp. 2083–2093, 2003.
- 4 J. M. Forbes, G. Lu, S. Bruinsma, S. Nerem, and X. Zhang, "Thermosphere density variations due to the 15–24 Apr. 2002 solar events from CHAMP/STAR accelerometer measurements," J. Geophys. Res., Vol. 110, A12S27, doi: 10.1029/2004JA010856, 2005.
- 5 T. Maruyama, "Extreme enhancement in total electron content after sunset on 8 Nov. 2004 and its connection with storm enhanced density," Geophys. Res. Lett., Vol. 33, L20111, doi: 10.1029/2006GL027367, 2006.
- 6 B. Tsurutani et al., "Global dayside ionospheric uplift and enhancement associated with interplanetary electric field," J. Geophys. Res., Vol. 109, doi: 10.1029/2003JA010342, 2004.
- 7 T. Maruyama, G. Ma, and M. Nakamura, "Signature of TEC storm on 6 Nov. 2001 derived from dense GPS receiver network and ionosonde chain over Japan," J. Geophys. Res., Vol. 109, doi: 10.1029/2004JA010451, 2004.
- 8 H. Jin and T. Maruyama, "Temporary Decrease in Daytime F-region Peak Electron Density due to Eastward Electric Field Penetration during Magnetic Storm," J. Geophys. Res., Vol. 113, A05305, doi: 10.1029/2006JA011928, 2008.
- 9 J. D. Huba, G. Joyce, and J. A. Fedder, "Sami2 is another model of the ionosphere (SAMI2): A new low-latitude ionosphere model," J. Geophys. Res., Vol. 105, pp. 23,035–23,053, 2000.



JIN Hidekatsu, Dr. Sci.
*Expert Researcher, Space Environment
Group, Applied Electromagnetic
Research Center
Upper Atmospheric Physics*

MARUYAMA Takashi, Ph.D. (Eng.)
*Executive Researcher
Upper Atmospheric Physics*